Video Article

Microfluidic Dry-spinning and Characterization of Regenerated Silk Fibroin Fibers

Qingfa Peng[1], Huili Shao[1], Xuechao Hu[1], Yaopeng Zhang[1]

[1]State Key Laboratory for Modification of Chemical Fibers and Polymer Materials, College of Materials Science and Engineering, Donghua University

Correspondence to: Yaopeng Zhang at zyp@dhu.edu.cn

URL: https://www.jove.com/video/56271
DOI: doi:10.3791/56271

Keywords: Chemistry, Issue 127, Dry-spinning, biomimetic, regenerated silk fibroin fiber, microfluidic, structure, synchrotron radiation

Date Published: 9/4/2017

Citation: Peng, Q., Shao, H., Hu, X., Zhang, Y. Microfluidic Dry-spinning and Characterization of Regenerated Silk Fibroin Fibers. *J. Vis. Exp.* (127), e56271, doi:10.3791/56271 (2017).

Abstract

The protocol demonstrates a method for mimicking the spinning process of silkworm. In the native spinning process, the contracting spinning duct enables the silk proteins to be compact and ordered by shearing and elongation forces. Here, a biomimetic microfluidic channel was designed to mimic the specific geometry of the spinning duct of the silkworm. Regenerated silk fibroin (RSF) spinning doped with high concentration, was extruded through the microchannel to dry-spin fibers at ambient temperature and pressure. In the post-treated process, the as-spun fibers were drawn and stored in ethanol aqueous solution. Synchrotron radiation wide-angle X-ray diffraction (SR-WAXD) technology was used to investigate the microstructure of single RSF fibers, which were fixed to a sample holder with the RSF fiber axis normal to the microbeam of the X-ray. The crystallinity, crystallite size, and crystalline orientation of the fiber were calculated from the WAXD data. The diffraction arcs near the equator of the two-dimensional WAXD pattern indicate that the post-treated RSF fiber has a high orientation degree.

Video Link

The video component of this article can be found at https://www.jove.com/video/56271/

Introduction

Spider and silkworm can produce outstanding silk fiber from aqueous protein solution at ambient temperature and pressure. Shearing and extensional flow can induce the formation of liquid crystal texture in the silk gland[1]. In recent years, there has been a great interest in mimicking the spinning process of the spider in order to produce high strength artificial fibers. However, large quantities of spider silk protein cannot be produced efficiently and economically by farming spiders due to cannibalism. Substantial amounts of silkworm silk can be obtained easily by farming. Otherwise, the silkworm and spider have a similar spinning process and amino acid composition. Therefore, silkworm silk fibroin is selected as a substitute to spin artificial animal silk by many researchers.

Spider and silkworm extrude protein solution through their spinning duct into fiber in air. The high stress forces generated along the spinning duct most likely stretch the silk fibroin molecules to a more extended conformation[2]. Artificial silk fibers have been spun using conventional wet spinning and dry-spinning processes[3,4], which do not take into account the fluid forces generated in the spinning duct.

First, microfluidic approaches were used to investigate the assembly of silk protein[5,6]. Then, microfluidic fabrication of RSF was studied via modeling the shearing and extensional forces[7,8]. Young's modulus and diameter of RSF fibers can be tuned by microfluidic wet spinning, but the tensile strength of drawn fiber was less than 100 MPa[7]. Finally, high strength RSF fibers were successfully prepared using the microfluidic dry-spinning method, but the diameter of the fiber is only 2 μm[8]. Recently, microfluidic wet spinning was successfully used in the production of high strength recombinant spider silk fiber. The post-spinning drawing in air improved the surface and internal defects of artificial fiber[9].

In this study, the improved microfluidic spinning process for RSF fiber is introduced. It aims to mimic the spinning process of silkworm silk, including the spinning dope, shearing forces, and dry-spinning process. This spinning method not only can produce high strength artificial silk fiber, but also can adjust the diameter of the fiber. Firstly, the RSF spinning dope was sheared and elongated in a biomimic channel with a second order exponential decay. Secondly, the influences of relative humidity (RH) on the fiber morphology and properties were studied in the microfluidic dry-spinning process[10]. Compared to the conventional spinning spinneret, our microfluidic system is highly biomimetic and can be used to produce high strength fiber from solutions at ambient temperature by the dry or wet spinning method.

Due to the high-resolution, high-brightness, and high-energy of the synchrotron radiation microfocus X-ray, it can be used to characterize the microstructure of a single fiber with a diameter of several micrometers[4,11,12,13,14]. Here, SR-WAXD technique was used to calculate the crystallinity, crystallite size and crystalline orientation of RSF fibers.

Protocol

CAUTION: Please consult all relevant material safety data sheets before use. Several of the chemicals used in preparing the molding are acutely toxic. Please use personal protective equipment (safety glasses, gloves, lab coat, full length pants, and closed-toe shoes).

1. Microfluidic Spinning of RSF Aqueous Solution

1. **Preparation of RSF aqueous spinning dope**[4,15,16]
    1. Degumming of silkworm cocoon
        1. Degum the *Bombyx mori* cocoons twice in Na_2CO_3 aqueous solutions (0.5 wt% in water) at 100 °C for 30 min each, and then wash the silk with deionized water to remove the sericin.
    2. Dissolving of degummed silkworm cocoon
        1. Dry the degummed cocoon silks in air; then dissolve the degummed cocoon silks in 9.0 M LiBr aqueous solution with a ratio of 1:10 (w/v) at 40 °C for 2 h. For example, add 10 mL LiBr per 1 gram silk (**Figure 1a**).
    3. Centrifuging and filtering
        1. Dilute the RSF solution 1.5 times by deionized water. Centrifuge and filter to remove impurities. Centrifuge the RSF solution in 250 mL bottles at 4 °C for 10 min at 1,234.8 x g. Filter the RSF solution using a 20 μm filter and a vacuum pump. Double filter paper bed is preferable considering the experimentation effect.
    4. Dialyzing
        1. Dialyze the RSF solution in deionized water at 5 °C for 3 days using a cellulose semipermeable membrane (MWCO: 14,000 ± 2,000). The total volume of RSF solution is about 1 L, loaded in 4 dialysis bags. Put these dialysis bags in the bucket, which is filled with 10 L reverse osmosis (RO) deionized water.
        NOTE: The pH value of deionized water should be higher than 6, to avoid gelation during the concentration process. The pH of deionized water did not require adjustment for this protocol.
    5. Concentrating
        1. Condense the RSF aqueous solution to 20 wt% by forced airflow at 5 °C. Add 3 M $CaCl_2$ aqueous solution into the RSF solution to 1.0 mmol/g Ca^{2+} final concentration; then concentrate by forced air flow to 38-47 wt%.
        2. Weigh one drop of RSF solution on a glass slide and then dry it for 2 h in an oven at 105 °C.
        NOTE: The weight percent of the remaining solid compared to the weight of the drop before drying is the total concentration of protein and $CaCl_2$. The RSF concentration is derived after deduction of the mass of $CaCl_2$. At least four repeated measurements were performed. Our previous studies showed that the concentration of Ca^{2+} greatly affected the rheological properties and spinnability of the RSF aqueous solutions. Meanwhile, the addition of Ca^{2+} prompted the limited formation of β-sheet and the aggregation of RSF[17]. In a native spinning dope, $CaCl_2$ is considered to play an important role during the storage of spinning dope to avoid gelation before spinning.[18]

2. **Preparation of microfluidic chip**[8,19]
    1. Preparing photomask
        1. Design the micro-channel in a CAD program. Print the CAD file to produce a high-resolution transparency[19].
    2. Preparing the mold
        1. Cleaning the glass slide
            1. In a chemical hood, boil the glass slide in the mixed solution of concentrated sulfuric acid and 30 vol% hydrogen peroxide solution (10:1) for 20 min on a hot plate.
            CAUTION: Sulfuric acid and hydrogen peroxide vapors are extremely toxic.
        2. Washing the glass slide
            1. Wash the glass slide using deionized water, and blow dry with high purity nitrogen.
        3. Coating film
            1. Coat the SU-8 photoresist on the glass slide by a custom-built coating device with a gap of 100 μm between the bottom surface of the coating bar and the upper surface of glass.
        4. Spin coating
            1. Spread the photoresist on the glass slide to form a uniform film using a spin coater at 40.3 x g for 30 s. The thickness of the uniform film is about 85 μm.
        5. Solidification
            1. Solidify the photoresist in an oven with a temperature controlling program. Elevate the temperature from room temperature to 65 °C at 2 °C/min and hold at 65 °C for 2 min. Continue to heat up from 65 °C to 95°C and hold at 95 °C for 15 min. Turn off the oven and cool down naturally to room temperature in the oven.
        6. Ultraviolet light exposure
            1. Expose the side of glass slide with the photoresist to ultraviolet light for 12 s using the transparency as a photomask by photolithography[19].

NOTE: The wavenumber of the ultraviolet light is 365 nm and the exposure energy is 273.6 mJ/cm^2.
CAUTION: Take proper safety measure while working with UV light and the oven.

7. Solidify the photoresist as described in step 1.2.2.5.
8. Developing
    1. Clean the photoresist ultrasonically in developer solution for 30 s. Wash the glass slide by isopropanol and developer, alternating between the two, until there is no precipitation on the glass slide.
9. Solidify the photoresist in an oven with a temperature controlling program. Elevate the temperature from room temperature to 170 °C at 2 °C/min and hold at 170 °C for 30 min. Turn off the oven and cool down naturally to room temperature in the oven.

3. Soft lithography
    1. Pour 8.8 g liquid polydimethylsiloxane (PDMS) pre-polymer over the mold and cure for 30 min at 65 °C, and 15 min at 80 °C. Liquid PDMS pre-polymer consists of PDMS and curing agent (typically at 10:1 (w/w)).
4. Punching
    1. Punch a hole through the PDMS replica at the beginning of the channel by drill. The diameter of the drill is 1.2 mm.
5. Sealing
    1. Seal the PDMS replica with the channel to a flat PDMS layer without pattern by an oxygen plasma treatment on the surfaces of the two PDMS layers.
    NOTE: The overall preparation process of the chip takes about 72 h.

3. **Fabrication of RSF fiber**
    1. Injection of spinning dope
        1. Inject the RSF spinning dope into the microchannel at 2 μL/min by a syringe pump.
    2. Environment regulation
        1. Adjust the relative humidity to 40 ± 5 RH% or 50 ± 5 RH% using a humidifier. At 40 ± 5 RH%, as-spun fiber solidified more quickly than 50 ± 5 RH%.
    3. Production of RSF fiber
        1. Touch the RSF drop by a pinpoint at the outlet of the microfluidic channel, draw RSF fiber into air, and then reel it onto a roller through a 10-cm air gap at a speed of 3 cm/s (**Figure 1b**).
    4. Store the RSF fibers in a sealed desiccator for 24 h.
    5. Fiber post-treatment
        1. Draw the as-spun fibers 4 times at 0.9 mm s^{-1} in 80 vol% ethanol solution by a custom-built machine, and then keep the drawn fiber fixed and immerse the fibers in the solution for 1 h. Because of this treatment, the length of the fiber was changed from originally 15 mm to 60 mm.
    6. Preparing the sample for characterization
        1. Fix the post-treated fibers on a paper frame with a 10-mm gauge length. At least 20 fibers are need for measurement, including in the tensile test, SEM, FTIR, and WAXS. The diameters of the post-drawn fibers range from 5 to 10 μm. **Figure 1** shows the schematic of the fiber production and WAXD characterization. The mechanical properties of the RSF fibers were examined by a material testing system at (25 ± 2) °C and (45 ± 5)% relative humidity. The extension rate and gauge length were 2 mm/min and 1 cm, respectively.

2. Synchrotron Radiation Characterization of Crystalline Structure of RSF Fiber

1. **Synchrotron radiation characterization**[4,13,17]
    1. Adjustment of beamline
        1. Adjust the wavelength of the X-rays and spot size to 0.07746 nm and 3 x 2 μm^2, respectively.
        NOTE: The protocol is performed using the BL15U1 beamline at the Shanghai Synchrotron Radiation Facility.
    2. Location of the X-ray spot
        1. Find the location of the X-ray spot.
        NOTE: The location of the X-ray spot is adjusted by the laboratory technician at the Synchrotron Radiation Facility.
    3. Testing of standard sample: Cerium dioxide (CeO_2)
        1. Test a standard sample CeO_2 powder. The CeO_2 powder was characterized to calculate the circle center and the distance from the sample to the detector.
    4. Sample preparation
        1. Fix the RSF filaments in parallel with each other on the paper frame with a 10 mm gauge length. Glue the paper frame on the testing stage.
        NOTE: Keep the fiber horizontal.
    5. SR-WAXD testing

1. Open the shutter
    1. Close the door of the beamline station after ensuring that there are no persons in the room. Open the shutter of X-ray beam source.

2. Focusing
    1. Move the fiber slightly until in focus. Adjust the location of fiber along the x, y, z direction remotely via a software (**Figure 1c**).

3. Sample exposure
    1. Move the fiber up and down remotely via a software, until it is on the X-ray spot. Press the start button on the software to expose the fiber to the X-ray beamline for 20 s (**Figure 1c**).

4. Background diffraction
    1. Test the diffraction of the air background with the exposure time of 20 s. Move the fiber away from the X-ray spot remotely via a software. Press the "start" button on the software to expose the X-ray beamline to "air medium" for 20 s.

2. **SR-WAXD data processing**[13]
    1. Software calibration
        1. Process the WAXD data using FIT2D (V12.077). Calibrate the circle center and the distance of sample-to-detector using the diffraction data of the CeO_2 powder.

    2. 2-D diffraction pattern
        1. Subtract the air background from the fiber diffraction pattern using FIT2D (V12.077).

    3. Crystallinity and crystallite size
        1. Integrate the diffraction intensity as a function of scattering angle 2θ. Perform deconvolution of the intensity integration by automated peak separation software (Version 4.12)[12]. The degree of crystallinity, x_c, was estimated from the relation:

$$X_c = \left(\frac{I_c}{I_c + I_a}\right)$$

        , where I_c is the sum of the integrated intensities of the crystalline peaks and I_a is the integrated intensity of the amorphous halo[4,11]. The integration of the WAXD patterns showed the peak width of the [200], [020], [002] reflections. The FWHM of these peaks were used to determine the crystallite size along the a, b, and c axes by using Scherrer's formula[4].

    4. Determination of the crystallite orientations
        1. Calculate the orientations of the crystallite and amorphous according to azimuthal integrations of (020) and (210) peaks[11]. The crystalline orientation can be calculated quantitatively according to Herman's orientation. Here, both (020) and (210) peaks were fitted with two Gaussian functions. The narrower one is for crystalline orientation and the other broader one is for the oriented amorphous material[13]. Here, the crystallite orientations of RSF fibers were compared using the full width at half maximum (FWHM) of azimuthal integrations (002) peaks.

Representative Results

High strength RSF fibers were successfully produced by using the microfluidic spinning method. The stress-strain curves and SEM images of the stretched RSF fibers C44R40 are shown in **Figure 2**. At least 10 fibers were measured in the tensile test. Stress-strain curves were chosen according to the average value of the breaking stress and strain of fibers. The WAXD data of the fibers are shown in **Figure 3**. The crystallinity and crystalline orientation were calculated according to the WAXD data. For sample designation, we use C and R to present the concentration of RSF in the spinning dope and the relative humidity, respectively. For example, the fibers spun from 44 wt% RSF spinning dope at 40 ± 5% RH was designated as C44R40, which was post-drawn at a draw ratio of 4. Other fibers were renamed as C44R50, C47R40, and C47R50 according to the same description.

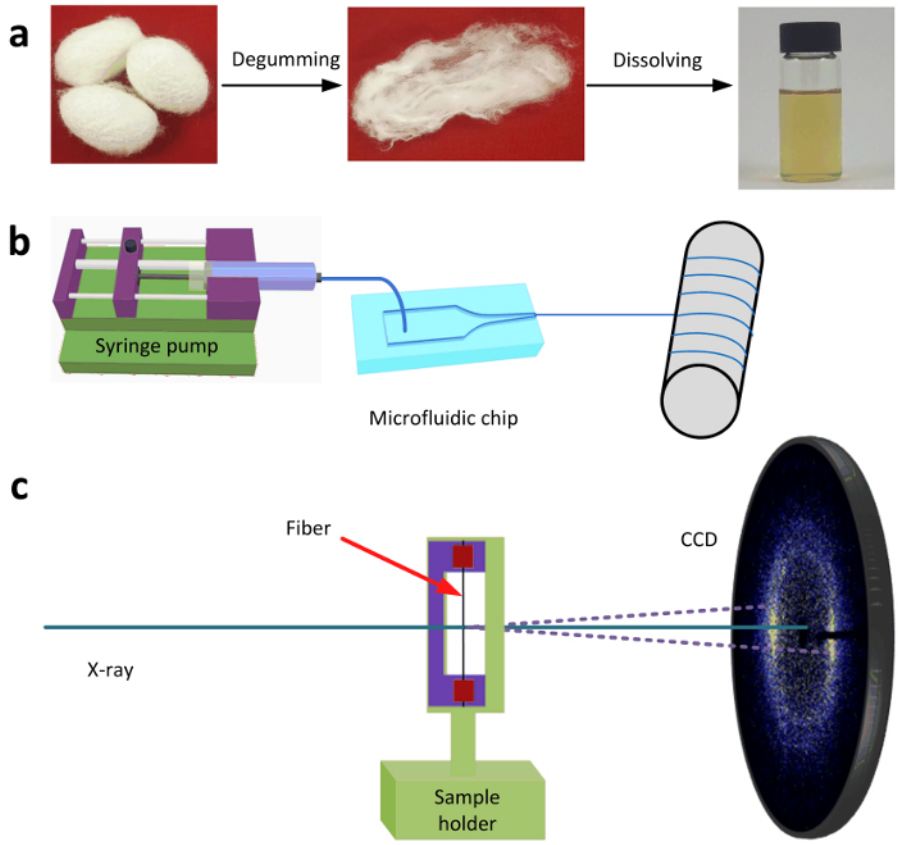

Figure 1: Schematic of the fiber production and structure characterization. (**a**) Preparation of RSF solution, (**b**) microfluidic spinning process of RSF fibers, (**c**) synchrotron radiation experimental setup of RSF single fiber. Please click here to view a larger version of this figure.

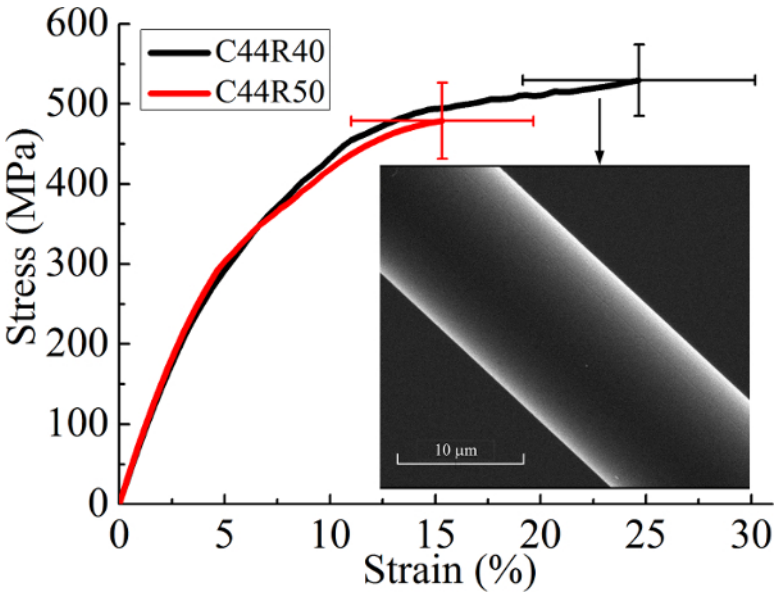

Figure 2: Stress-strain curves of post-treated RSF fibers. Insert shows SEM image of C44R40. Scale bar = 10 μm. This figure has been modified from[10]. Please click here to view a larger version of this figure.

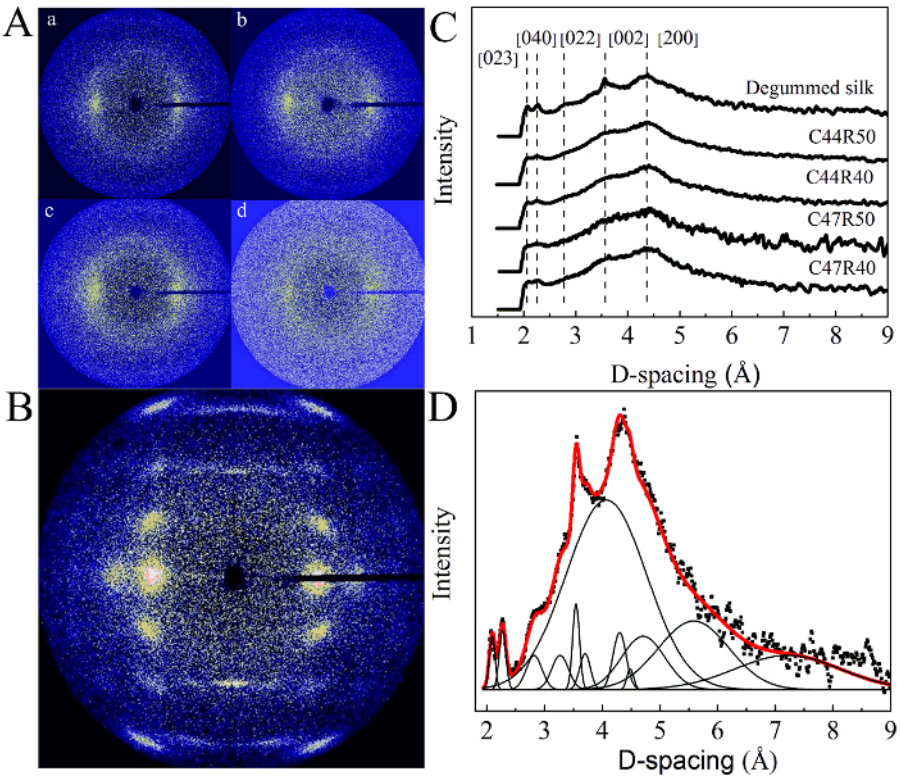

Figure 3: SR-WAXD data of post-treated RSF fibers. (**A**) Two dimensional WAXD patterns of post-treated RSF single fibers: (**a**) C44R40, (**b**) C44R50, (**c**) C47R40, (**d**) C47R50, and (**B**) degummed *B. mori* silk; (**C**) One dimensional WAXD data of post-treated RSF fibers and degummed *B. mori* silk, which was performed at peak deconvolution in (**D**). This figure has been modified from reference[10]. Please click here to view a larger version of this figure.

Discussion

During the dialysis of the RSF solution, the pH value is critical for the following concentration process. If the pH value of the deionized water is smaller than 6, the RSF solution will be easier to gel during the concentration process. To avoid gelation, $CaCl_2$ is added to the RSF solution. The concentration of $CaCl_2$ is 1 mmol per weight of RSF.

Our previous work demonstrated the possibility of microfluidic dry-spinning of an RSF aqueous solution[8]. The geometry of the microfluidic channel was a simplified single-stage exponential function. For spider and silkworm, spinning dopes were draw down through a two-stage exponential regression spinning duct before fiber formation[1,20]. Here, the geometry of the microfluidic channel was designed by mimicking the second order exponential decay function of the silkworm spinning duct[1]. The width of the microfluidic channel decreases from an initial width of 2,065 μm to the terminal width of 265 μm, and the length of the elongation channel is 21.5 mm. In the previous article, the diameter of the drawn RSF fiber was 2 μm. Thus, a bundle of RSF threads had to be used for the mechanical test and structure characterization[8].

The experiment shows that RSF concentration and relative humidity affect the diameter and microstructure of the RSF fibers in the dry spinning process. The RSF fiber spun at 40% RH shows a larger diameter and more crystalline structures than the fiber spun at 50% RH. However, the fiber spun at 50% RH has a higher crystalline orientation than that spun at 40% RH. The results might be related to evaporation rates of water at different humidities. A higher evaporation rate of water at 40% RH improves the intramolecular interactions and facilitates the fast phase transition of silk fibroin from sol-gel to solid silk fiber. A lower evaporation rate of water at 50% RH leads to a higher content of residue water in the solidified fiber. As a small molecular lubricant, the water facilitates the silk fibroin orientation and makes the partially solidified fiber to be stretched to finer fibers. This process helps us understand how water influences the formation of silk fibers during native spinning process.

The mechanical properties of post-treated RSF fibers are better than those of degummed silks[4]. After post-treatment, crystallinities of the fibers were drastically increased. The FWHM of the post-treated RSF fiber is smaller than that of as-spun fiber. It indicates that post-treatment improves the orientation of crystallites along the fiber axis. However, the complexity of the post-treatment process limits the mass production of RSF fibers with high strength.

Compared to a conventional spinneret, the microfluidic channel is well suited to mimic the geometry of a natural silk gland. Meanwhile, the microfluidic spinning was used to produce recombinant spider silk with outstanding mechanical properties[9]. Shearing and elongational sections were integrated in the microfluidic spinning chip to induce assembly and orientation of the protein molecules and fibrils. Therefore, the microfluidic spinning is promising in the production of high-performance animal silks, as well as other synthetic fibers from solution. However, the microfluidic spinning method can only produce single filaments and it cannot afford high production of artificial fibers.

Disclosures

The authors have nothing to disclose.

Acknowledgements

This work is sponsored by the National Natural Science Foundation of China (21674018), the National Key Research and Development Program of China (2016YFA0201702 /2016YFA0201700), and the "Shuguang Program" supported by Shanghai Education Development Foundation and Shanghai Municipal Education Commission (15SG30), DHU Distinguished Young Professor Program (A201302), the Fundamental Research Funds for the Central Universities, and the 111 Project (No.111-2-04).

References

1. Asakura, T. *et al.* Some observations on the structure and function of the spinning apparatus in the silkworm Bombyx mori. *Biomacromolecules.* **8** (1), 175-181 (2007).
2. Vollrath, F., & Knight, D. P. Liquid crystalline spinning of spider silk. *Nature.* **410** (6828), 541-548 (2001).
3. Zhou, G. Q., Shao, Z. Z., Knight, D. P., Yan, J. P., & Chen, X. Silk Fibers Extruded Artificially from Aqueous Solutions of Regenerated Bombyx mori Silk Fibroin are Tougher than their Natural Counterparts. *Adv Mater.* **21** (3), 366-370 (2009).
4. Sun, M. J., Zhang, Y. P., Zhao, Y. M., Shao, H. L., & Hu, X. C. The structure-property relationships of artificial silk fabricated by dry-spinning process. *J Mater Chem.* **22** (35), 18372-18379 (2012).
5. Martel, A. *et al.* Silk Fiber Assembly Studied by Synchrotron Radiation SAXS/WAXS and Raman Spectroscopy. *J Am Chem Soc.* **130** (50), 17070-17074 (2008).
6. Rammensee, S., Slotta, U., Scheibel, T., & Bausch, A. R. Assembly mechanism of recombinant spider silk proteins. *P Natl Acad Sci USA.* **105** (18), 6590-6595 (2008).
7. Kinahan, M. E. *et al.* Tunable silk: using microfluidics to fabricate silk fibers with controllable properties. *Biomacromolecules.* **12** (5), 1504-1511 (2011).
8. Luo, J. *et al.* Tough silk fibers prepared in air using a biomimetic microfluidic chip. *Int J Biol Macromol.* **66** 319-324 (2014).
9. Peng, Q. F. *et al.* Recombinant spider silk from aqueous solutions via a bio-inspired microfluidic chip. *Sci Rep.* **6** (2016).
10. Peng, Q. F., Shao, H. L., Hu, X. C., & Zhang, Y. P. Role of humidity on the structures and properties of regenerated silk fibers. *Prog Nat Sci-Matter.* **25** (5), 430-436 (2015).
11. Sampath, S. *et al.* X-ray diffraction study of nanocrystalline and amorphous structure within major and minor ampullate dragline spider silks. *Soft Matter.* **8** (25), 6713-6722 (2012).
12. Martel, A., Burghammer, M., Davies, R. J., & Riekel, C. Thermal Behavior of Bombyx mori silk: Evolution of crystalline parameters, molecular structure, and mechanical properties. *Biomacromolecules.* **8** (11), 3548-3556 (2007).
13. Pan, H. *et al.* Nanoconfined crystallites toughen artificial silk. *J Matter Chem B.* **2** (10), 1408-1414 (2014).
14. Zhang, C. *et al.* Microstructural evolution of regenerated silk fibroin/graphene oxide hybrid fibers under tensile deformation. *Rsc Adv.* **7** (6), 3108-3116 (2017).
15. Wei, W. *et al.* Bio-inspired capillary dry spinning of regenerated silk fibroin aqueous solution. *Mat Sci Eng C-Mater.* **31** (7), 1602-1608 (2011).
16. Jin, Y., Zhang, Y. P., Hang, Y. C., Shao, H. L., & Hu, X. C. A simple process for dry spinning of regenerated silk fibroin aqueous solution. *J Mater Res.* **28** (20), 2897-2902 (2013).
17. Jin, Y., Hang, Y. C., Zhang, Y. P., Shao, H. L., & Hu, X. C. Role of Ca2+ on structures and properties of regenerated silk fibroin aqueous solutions and fibres. *Mater Res Innov.* **18** 113-116 (2014).
18. Koh, L. D. *et al.* Structures, mechanical properties and applications of silk fibroin materials. *Prog Polym Sci.* **46** 86-110 (2015).
19. McDonald, J. C., & Whitesides, G. M. Poly(dimethylsiloxane) as a material for fabricating microfluidic devices. *Accounts Chem Res.* **35** (7), 491-499 (2002).
20. Knight, D. P., & Vollrath, F. Liquid crystals and flow elongation in a spider's silk production line. *P Roy Soc B-Biol Sci.* **266** (1418), 519-523 (1999).

